

Temperature fields in the fusion zone induced by a moving electron beam

C. Y. Ho^{1,*} and Y. C. Lee²

¹*Department of Mechanical Engineering, Hwa Hsia Institute of Technology*

²*Department of Architecture and Landscape, National Taitung Junior College*

(Manuscript Received May 31, 2007; Revised August 30, 2007; Accepted September 30, 2007)

Abstract

An analytical model is developed to investigate the heat transfer in the fusion zone during electron-beam welding. The keyhole produced by an electron-beam is assumed to be a paraboloid of revolution and the profile of the intensity of an electron beam is supposed to be Gaussian distribution. In order to obtain an analytical solution, a quasi-steady heat conduction Eq. is utilized to analyze the heat transfer in the workpiece and the parameter approximating convection is proposed to account for the effect of heat convection of molten metal. Considering the momentum balance at the bottom of the keyhole but neglecting the absorption in the plume, an analytical solution is obtained for semi-infinite workpieces. The effects of various parameters on the temperature distribution are also discussed in this study.

Keywords: Temperature distribution; Fusion zone; Electron beam

1. Introduction

Heat transfer analysis is of crucial importance in materials manufacturing and processing [1-2]. This is also due to the availability of new materials and to the use of innovative processes employing laser and electron beam. These high power beams are now widely used in many applications, such as welding, drilling, cutting, heat treating of metals and manufacturing of electronic components. It is, therefore, necessary to study the conductive thermal fields induced in the solid by a moving heat source.

Most theoretical studies were made to the infinite or semi-infinite body. One of the first analytical solutions was derived by Jaeger [3] for the temperature distribution in a semi-infinite solid with a

surface moving heat source. Rosenthal [4] developed the theory for the moving heat source and presented the exact solutions for differently shaped moving spots on both semi-infinite and finite bodies. The same solutions for a semi-infinite solid were obtained by Carslaw and Jaeger [5] by using the heat source method.

As far as a Gaussian distribution of the laser and electron beam heat flux is assumed, solutions to the temperature field induced in semi-infinite solids by a moving circular Gaussian heat source have been derived by several authors. Cline and Anthony [6] correlated the cooling rate and the melting depth to the size, the velocity and the power of the spot. Chen and Lee [7] took into account the effects of the scanning velocity, the beam radius and the beam shape on the temperature profiles. Sanders [8] presented a general solution and found the conditions under which the solution as a function of its normalized

*Corresponding author. Tel.: +886 2 89415131, Fax.: +886 2 29436521
E-mail address: hcy2126@cc.hwh.edu.tw

velocity can be used; the author extended analysis to a moving Gaussian pulsed heat source. The same problem was analyzed by Modest and Abakians [9]. Nissim et al. [10] presented an analytical solution for a moving elliptical Gaussian heat source, which accounted for the temperature dependence of thermal conductivity. Their model was generalized by a numerical algorithm set up by Moody and Hendel [11].

When the order of magnitude of penetration depth is the same as that of the body thickness, the solid can no longer be assumed as semi-infinite one. Pittaway [12] solved the temperature distribution in an adiabatic thin plate with either stationary or moving circular Gaussian heat source. For the same heat sources Lolov [13] derived the solution to the three dimensional linear problem in a finite depth and indefinite width adiabatic body. Tsai and Hou [14] analyzed for a solid whose dimension along the direction perpendicular to that of the motion was finite, the thermal characterization of the welding both at steady-state and transient conditions. The same problem was solved by Kar and Mazumder [15]; their model allowed the determination of the transient three-dimensional temperature distribution in a solid whose thermophysical properties, except the thermal diffusivity, were assumed to be time dependent. Manca [16] developed an analytical solution to the three-dimensional quasi-stationary problem in a finite depth and width with a circular Gaussian moving heat source at the body surface.

The line-source model in its pristine form has certain defects. These are: (1) infinite temperatures occurred near the sources; (2) the distribution of incident flux was not taken into account. Wei et al. [17, 18] found that the distribution of incident fluxes is an important factor affecting the depth of penetration; (3) vertical heat transport was neglected; (4) momentum balance was not taken into account. In order to avoid weaknesses of the line-source model, Wei and Shian [19] proposed a three-dimensional analytical model around the cavity produced by a moving distributed high-intensity beam, which considered the momentum balance at the cavity base and did not result in infinite temperature. On the basis of the model proposed by Wei and Shian, this work provided an analytical solution accounting for the effect of beam parameters on the temperature field.

2. Analysis

2.1 Governing equation

A workpiece is moved with a constant speed relative to the electron beam as sketched in Fig. 1. As the base material reaches the energy beam location, it is melted and flows in a thin layer around a vapour-supported cavity to the rear where it cools and solidifies.

A heat conduction Eq. is utilized to describe this quasi-steady-state process.

$$-\hat{U} \frac{\partial \hat{T}}{\partial \hat{x}} = \alpha \left(\frac{\partial^2 \hat{T}}{\partial \hat{x}^2} + \frac{\partial^2 \hat{T}}{\partial \hat{y}^2} \right) + \alpha_z \left(\frac{\partial^2 \hat{T}}{\partial \hat{z}^2} \right) \quad (1)$$

For welding with a moving heat source the geometry becomes slightly asymmetric [20]. The cavity, however, can be roughly observed to be a paraboloid of revolution near the cavity base [21, 22], especially for a deep and narrow cavity. Hence, the cavity is idealized by a paraboloid of revolution and a curvilinear orthogonal parabolic coordinate $\xi\eta\phi$ system can be used effectively. Introducing the following transforms

$$x = \frac{\hat{x}}{\hat{\sigma}} = \frac{2\sqrt{\xi\eta} \cos \phi}{P_e} \quad (2)$$

$$y = \frac{\hat{y}}{\hat{\sigma}} = \frac{2\sqrt{\xi\eta} \sin \phi}{P_e} \quad (3)$$

$$z = \frac{\hat{z}}{\hat{\sigma}} = \frac{(\xi - \eta)}{P_e \sqrt{S}} \quad (4)$$

$$\theta = \frac{\hat{T} - T_\infty}{\hat{T} - T_m} \quad (5)$$

$$\Theta = \theta \exp[\sqrt{\xi\eta} \cos \phi] \quad (6)$$

where Peclet number and the parameter approximating convection, respectively, are defined as $P_e \equiv \hat{U}\hat{\sigma}/\hat{\alpha}$ and $P_e \equiv \hat{\alpha}/\hat{\alpha}_z$. \hat{U} , $\hat{\sigma}$, $\hat{\alpha}$, and $\hat{\alpha}_z$ correspondingly denote the dimensional workpiece speed, energy distribution parameter, liquid diffusivity, and enhanced diffusivity in vertical direction. ξ and η are the parabolic coordinates. The dimensionless form of Eq. (1) expressed in parabolic coordinate system is

$$\frac{4}{\xi + \eta} \left[\frac{\partial}{\partial \xi} \left(\xi \frac{\partial \Theta}{\partial \xi} \right) + \frac{\partial}{\partial \eta} \left(\eta \frac{\partial \Theta}{\partial \eta} \right) + \frac{1}{4} \left(\frac{1}{\xi} + \frac{1}{\eta} \right) \frac{\partial^2 \Theta}{\partial \phi^2} \right] = \Theta \quad (7)$$

Thermal diffusivity is not isotropic in order to account for the convection. Since the flow of liquid enhances energy transport, the diffusivity in the flow direction is increased by a constant multiple of around five [23, 24]. Therefore, the parameter approximating convection, S , is proposed.

2.2 Incident energy flux and boundary conditions

The profile in any horizontal cross section for an electron beam is a Gaussian distribution. This was confirmed by Hicken et al. [25] by measuring distributions of incident fluxes at vertical distances that deviated from the focal spot of an electron beam. Therefore the energy flux of electron beam can be described by

$$q_j = \frac{3}{\pi\sigma^2} e^{-3(\frac{r}{\sigma})^2} \tag{8}$$

where 3 is selected to assure 95 percent of incident

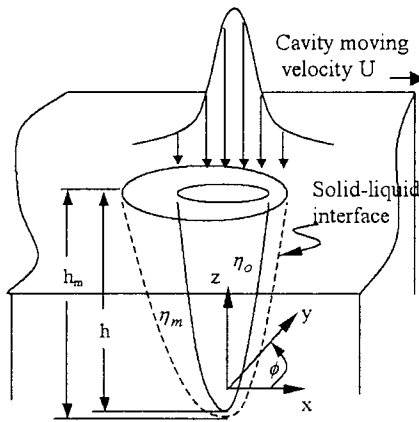


Fig. 1. Schematic diagram of physical model and coordinate system.

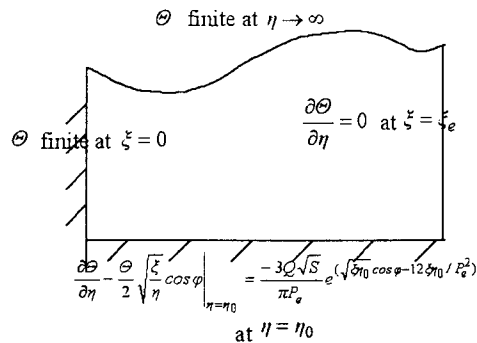


Fig. 2. Boundary conditions.

energy located within the energy-distribution radius. Energy losses due to evaporation can be neglected by comparison with incident beam energy and it is assumed that the incident energy flux is totally absorbed by the cavity. An energy balance between incident flux and conduction on the cavity wall ($\eta = \eta_0$) then yields

$$\frac{\partial\Theta}{\partial\eta} - \frac{\Theta}{2} \left. \frac{\sqrt{\xi}}{\eta} \cos\phi \right|_{\eta=\eta_0} = \frac{-3Q\sqrt{S}}{\pi P_e} \exp(\sqrt{\xi}\eta_0 \cos\phi - \frac{12\xi\eta_0}{P_e^2}) \tag{9}$$

where the dimensionless beam power Q is defined as $\hat{Q}/\hat{k}_l\hat{\sigma}(\hat{T}_m - \hat{T}_\infty)$. The second term on the left-hand side of Eq. (9) is ignored because no error occurs at a location of either an angle of $\pi/2$ or the cavity base where the incident flux is the highest. Although errors increase as the workpiece surface is approached, temperatures predicted are still acceptable. The reason for this is that energies impinging on this region have a large incident angle so that the intensity is reduced. It is also assumed to be negligible for heat loss to ambient air from the workpiece surface outside the cavity. Therefore, the adiabatic condition is employed on the workpiece surface. The dimensionless temperature Θ is finite at the cavity base ($\xi = 0$) and at $\eta \rightarrow \infty$. Local thermodynamic equilibrium is assumed at the base of the cavity. The momentum balance between the vapor pressure and pressure due to surface tension at the cavity base is required to determine the coordinate η_0 of the cavity surface [26]. This yields

$$\eta_0 = \frac{Pe[1 + Y(\theta_b - 1)]}{P} e^{\frac{H(\theta_b - \theta_B)}{(\theta_b + \theta_x)(\theta_b + \theta_x)}} \tag{10}$$

where θ_B and θ_b , respectively, represent the dimensionless temperature at cavity base and boiling. Other dimensionless parameters in Eq. (10) are defined as

$$Y = \frac{(\hat{T}_m - \hat{T}_\infty)d\hat{\gamma}/d\hat{T}}{\hat{\gamma}_m} \tag{11}$$

$$P = \frac{\hat{p}_b\hat{\sigma}}{\hat{\gamma}_m} \tag{12}$$

$$H = \frac{\hat{h}_{lg}}{R(\hat{T}_m - \hat{T}_\infty)} \tag{13}$$

\hat{p}_b is the vapor pressure at boiling and is evaluated by the Clausius-Clapeyron Eq.. $\hat{\gamma}$ is surface tension and is assumed to be a linearly decreasing function of temperature. When the temperature arrives at the melting point, $\hat{\gamma}$ is equal to $\hat{\gamma}_m$. \hat{h}_{lg} is the latent heat of evaporation and \hat{R} is gas constant.

2.3 Analytical solution

Eq. (7) with the boundary conditions as shown in Fig. 2 can be solved by using the separation-of-variables method.

Introducing the dependent variable $\Theta(\xi, \eta, \phi) = \Omega(\xi)\Lambda(\eta)\Pi(\phi)$ into Eq. (7), three ordinary differential Eqs are obtained

$$\frac{d^2\Omega}{d\xi^2} + \frac{1}{\xi} \frac{d\Omega}{d\xi} + \left(-\frac{m^2}{4\xi^2} + \frac{n}{\xi} - \frac{1}{4}\right)\Omega = 0 \tag{14}$$

$$\frac{d^2\Lambda}{d\eta^2} + \frac{1}{\eta} \frac{d\Lambda}{d\eta} + \left(-\frac{m^2}{4\eta^2} - \frac{n}{\eta} - \frac{1}{4}\right)\Lambda = 0 \tag{15}$$

$$\frac{d^2\Pi}{d\phi^2} + m^2\Pi = 0 \tag{16}$$

In order to satisfy the symmetric condition at the welds centerline and finite temperature at the cavity base and infinity, the forms of solutions of Eqs. (14)-(16) correspondingly yield

$$\Omega \sim \xi^{-\frac{m}{2}} e^{-\frac{\xi}{2}} L_{p-1}^m(\xi) \tag{17}$$

$$\Lambda \sim \eta^{\frac{m}{2}} e^{-\frac{\eta}{2}} \Psi(m+p, m+1, \eta) \tag{18}$$

$$\Pi \sim \cos m\phi \quad (m=0,1,2,3,\dots) \tag{19}$$

where the functions L_p^m and Ψ are the Laguerre function and confluent hypergeometric function of the second kind, respectively. Therefore, a general solution of Eq. (7) is

$$\Theta = e^{-\frac{\xi+\eta}{2}} \sum_{m=0}^{\infty} \sum_{p_i} C_{m,p_i} (\xi\eta)^{\frac{m}{2}} L_{p_i}^m(\xi) \Psi(m+p_i, m+1, \eta) \cos m\phi \quad \text{for } \eta \geq \eta_0 \tag{20}$$

Substituting Eq. (20) into Eq. (9), multiplying the resulting Eq. by $\cos(m\phi)$, $\xi^{m/2}$, $\exp(-\xi/2)$, and $L_{p-1}^m(\xi)$, integrating over ϕ and ξ [27], and using the orthogonal properties of cosine and Laguerre

functions the coefficients give

$$C_{m,p_i} = \left(\frac{1}{2}\right)^{\delta_{m0}-1} \int_0^{\xi_0} \xi^{\frac{m}{2}} e^{-\frac{\xi}{2}} \frac{\Gamma(m+1)\Gamma(p_i+1)}{\Gamma(m+p_i+1)} L_{p_i}^m(\xi) e^{-\frac{12\xi\eta_0}{Pe^2}} I_m(\sqrt{\xi\eta_0}) \cos m\phi d\xi / \eta_0^2 e^{-\frac{m}{2} \frac{\eta_0}{2}} \tag{21}$$

$$\left[\left(\frac{m}{2\eta_0} - .5\right)\psi + \frac{d\psi}{d\eta} \right]_{\eta_0} Norm(m, p_i)$$

where Norm is defined as

$$Norm(m, p_i) \equiv \int_0^{\xi_0} (L_{p_i}^m)^2 d\xi$$

The modified Bessel function of the first kind I_m and gamma function Γ appear in the case. The temperature predicted by using $m=0$ is sufficiently accurate with errors of less than 3 %.

2.4 The solution procedure

The solution procedure follows as

1. An initial η_0 is guessed.
2. The base temperature is calculated from Eqs. (20) and (21).
3. An improved η_0 is obtained from Eq. (10).
4. Steps 2 and 3 are repeated until η_0 converges.
5. The second law of thermodynamics is used to uniquely determine η_0 .

Since there exist two cavities where bases satisfy balances of momentum and energy [19], step 5 is required. Applying the second law of thermodynamics, the correct cavity is the one whose base temperature is increased with the dimensionless beam power.

3. Results and discussion

This paper provided an analytical model to predict the temperature field of an electron beam irradiating on a semi-infinite workpiece. The cavity shape is assumed to be a paraboloid of revolution. This model was formulated in a parabolic coordinate system attached to a workpiece moving with constant speed and therefore, can be considered as a quasi-steady-state problem. In order to account for the enhanced diffusivity in the flow or approximately vertical direction, the S was implemented into this thermal model. The momentum balance at cavity base is used

to determine the cavity depth. The effects of Peclet number, parameter approximating convection and beam power on temperature field were investigated.

The predicted beam power per unit of penetration versus solid Peclet number for welding workpiece of SS 304 is shown in Fig. 3 and agrees with experimental data obtained by Hicken et al. [25]. Fig. 3 also indicates that the beam power per unit of penetration increases as the moving speed for workpiece or an electron beam becomes fast or the liquid-to-solid diffusivity ratio (Λ) decreases.

The isothermal lines in heat-affected zone for $Pe=0.25$, $S=0.08$, and $Q=60$ are sketched in Fig. 4. The paraboloid of revolution-shaped cavity is also shown in this Fig. The dimensionless temperatures greater and lower than one indicate fusion zone and solidification zone, respectively. Based on the direction of cavity movement, fusion zone is smaller ahead of the cavity (+x) than behind the cavity (-x). The bottom of fusion zone deviates the z axis due to

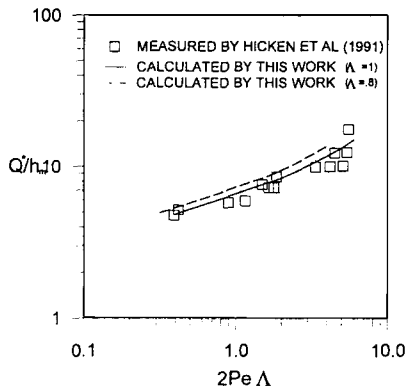


Fig. 3. Variation of the predicted and measured beam power per unit of penetration with solid Peclet number for different liquid-to-solid diffusivity ratios.

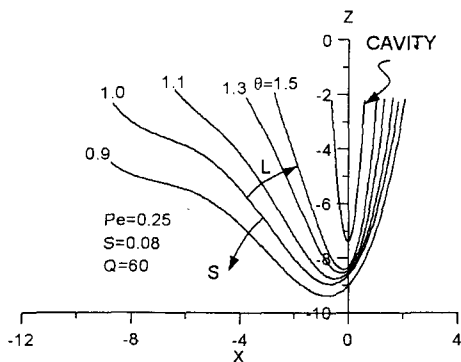


Fig. 4. Isothermal line in heat-affected zone for $Pe=0.25$, $S=0.08$, and $Q=60$.

the moving workpiece or electron-beam. The isothermal lines near workpiece surface expand toward outside. This is consistent with the observed phenomenon.

Fig. 5 shows isothermal lines in heat-affected zone for $Pe=0.125$, $S=0.08$, and $Q=60$. Compared with Fig. 4, the moving velocity of workpiece or electron-beam is slower in Fig. 5 which indicates the deeper cavity and fusion zone. The size differences of fusion zones between ahead of cavity and behind cavity decrease due to the slowly moving velocity. The deviations from z axis for the bottom of fusion zone and the fusion zone at workpiece surface are also reduced in the same reason.

The effect of the S on temperature distribution is presented by the comparison of Fig. 4 with Fig. 6. The large S means that the effective diffusivity in z direction decreases relative to other directions. There-

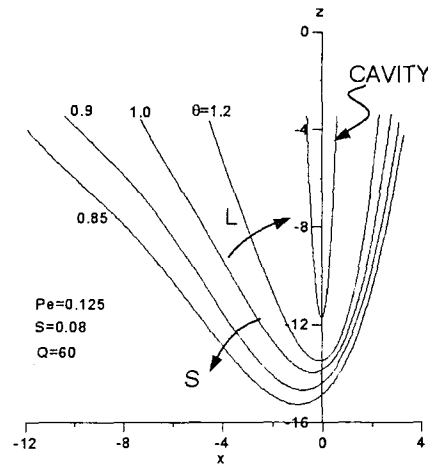


Fig. 5. Isothermal line in heat-affected zone for $Pe=0.125$, $S=0.08$, and $Q=60$.

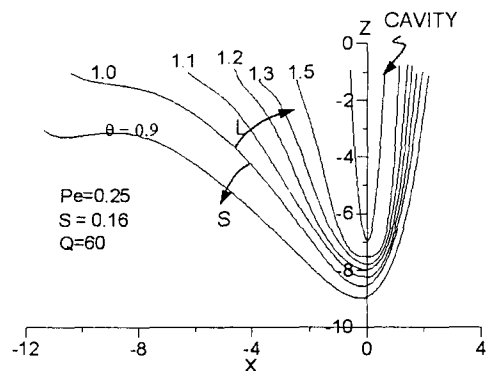


Fig. 6. Isothermal line in heat-affected zone for $Pe=0.25$, $S=0.16$, and $Q=60$.

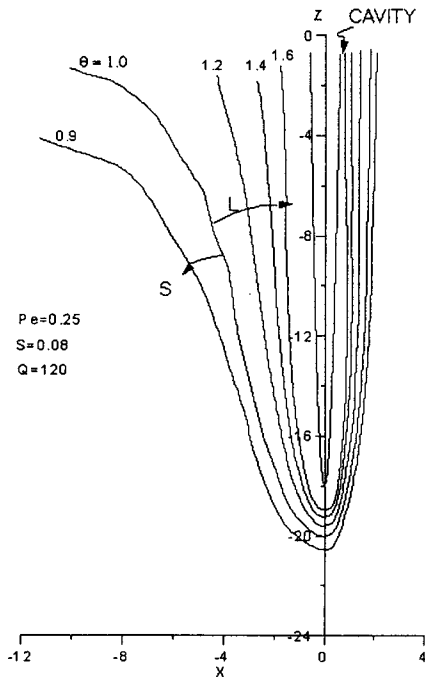


Fig. 7. Isothermal line in heat-affected zone for $Pe=0.25$, $S=0.08$, and $Q=120$.

fore the heat dissipation along z direction from the bottom of cavity to workpiece surface becomes smaller. This results in much more heat available at the bottom of cavity to melt the workpiece and obtain the deeper cavity and fusion zone. However compared with Fig. 4, the range of the fusion zone at workpiece surface insignificantly changes and the deviation of the bottom of fusion zone from z axis decreases in Fig. 6. From Figs. 5 and 6 it can be also noted that the effect of moving velocity on temperature field is more obvious than the S .

Fig. 7 reveals that higher power of incident electron-beam induces the deeper cavity and fusion zone. The shapes of fusion zone and cavity also agree with the experimental observation of deep penetration. Compared with the shallow cavity and fusion zone as Figs. 4 and 6, the isothermal line for deep penetration is more symmetric to z axis. Deep and narrow fusion zone is obtained in this case.

4. Conclusions

An analytical model is proposed to demonstrate the effects of Peclet number, parameter approximating convection and beam power on temperature field. The predicted beam power per unit of penetration versus

solid Peclet number for welding workpiece of SS 304 agrees with experimental data. The slow velocity of movement, large parameter approximating convection and high beam power give rise to deep cavity and fusion zone. The influence of beam power on temperature field is most obvious among them.

References

- [1] R.K. Shah, H.Md. Roshan, V.M.K. Sastri, K.A. Padmanabhan, Thermomechanical aspect of manufacturing and materials processing, Hemisphere, Washington, DC, (1992).
- [2] I. Tanasawa, N. Lior, Heat and mass transfer in materials processing, Hemisphere, Washington, DC (1992).
- [3] J.C. Jaeger, Moving sources of heat and temperature at sliding contacts, Proceedings of the Royal Society of N. S. W., 76 (1942) 203-224.
- [4] D. Rosenthal, The theory of moving sources of heat and its application to metal treatments, Trans. ASME J. Heat Transfer. 68 (1946) 849-866.
- [5] H.S. Carslaw, J.C. Jaeger, Conduction of heat in solids (2nd Edn), Oxford University Press, Oxford (1959).
- [6] H.E. Cline, T.R. Anthony, Heat treating melting material with a scanning laser or electron beam, J. Appl. Phys. 48 (1977) 3895-3900.
- [7] I. Chen, S. Lee, Transient temperature profiles in solids heated with scanning laser, J. Appl. Phys. 54 (1983) 1062-1066.
- [8] D.J. Sanders, Temperature distributions produced by scanning gaussian laser beam, Appl. Opt. 23 (1984) 30-35.
- [9] M.F. Modest, H. Abakians, Heat conduction in a moving semi-infinite solid subjected to pulsed laser irradiation, J. Heat Transfer. 108 (1986) 597-601.
- [10] Y. Nissim, A. Lietoila, R.B. Gold, J.F. Gibbons, Temperature distributions produced in semiconductors by a scanning elliptical or circular CW laser beam, J. Appl. Phys. 51 (1980) 274-279.
- [11] J.E. Moody, R.H. Hendel, Temperature profiles induced by a scanning CW laser beam, J. Appl. Phys. 53 (1982) 4364-4371.
- [12] L.G. Pittaway, The temperature distributions in thin foil and semi-infinite targets bombarded by an electron beam, Br. J. Appl. Phys. 15 (1964) 967-982.
- [13] N. Lolov, Temperature field with distributed moving heat source. International Institute of Welding, Study Group 212, Doc. 212-682-87 (1987).

- [14] C.L. Tsai, C.A. Hou, Theoretical analysis of weld pool behavior in the pulsed current GTAW process, *J. Heat Transfer*. 110 (1988) 160-165.
- [15] A. Kar, J. Mazumder, Three-dimensional transient thermal analysis for laser chemical vapor deposition on uniformly moving finite slabs, *J. Appl. Phys.* 65 (1989) 2923-2933.
- [16] O. Manca, B. Morrone, V. Naso, Quasi-steadystate three-dimensional temperature distribution induced by a moving circular gaussian heat source in finite depth solid, *Int. J. Heat Mass Transfer*. 38 (1995) 1305-1315.
- [17] P.S. Wei, J.Y. Ho, Energy considerations in high-energy beam drilling, *International J. of Heat and Mass Transfer*. 33 (1990) 2207-2217.
- [18] P.S. Wei, T.W. Lii, Electron beam deflection when welding dissimilar metals, *ASME J. of Heat Transfer*. 112 (1990) 714-720.
- [19] P.S. Wei, M.D. Shian, Three-dimensional analytical temperature field around the welding cavity produced by a moving distributed high-intensity beam, *ASME J. of Heat Transfer*. 115 (1993) 848-856.
- [20] P.S. Wei, T.H. Wu, Y.T. Chow, Investigation of high-intensity beam characteristics on welding cavity shape and temperature distribution, *Trans. ASME J. Heat Transfer*. 112/1 (1990) 163-169.
- [21] D.A. Schauer, W.H. Giedt, Prediction of electron beam welding spiking tendency, *Welding J.* 57 (1978) 189-195.
- [22] D.A. Schauer, W.H. Giedt, S.M. Shintaku, Electron beam welding cavity temperature distributions in pure metals and alloys, *Welding J.* 57 (1978) 127-133.
- [23] C. Gau, R. Viskanta, Melting and solidification of a metal system in a rectangular cavity, *International J. of Heat and Mass Transfer*, 27 (1984) 113-123.
- [24] W.H. Giedt, X.C. Wei, S.R. Wei, Effect of surface convection on stationary gta weld zone temperature, *Welding J.* 63 (1984) 376-383.
- [25] G.K. Hicken, W.H. Giedt, A.E. Bentley, Correlation of joint penetration with electron beam current distribution, *Welding J.* 70 (1991) 695-755.
- [26] P.S. Wei, Y.T. Chow, Beam focusing characteristics and alloying element effects on high-intensity electron beam welding, *Metallurgical Transactions B.* 23 (1992) 81-90.
- [27] I.S. Gradshteyn, I.M. Ryzhik, *Table of integrals, Series, and Products*, edited by Jeffrey, A., and translated from the Russian by Scripta Technica, Inc., England, 482 and 847 (1980).